Effect of dilution in asymmetric recurrent neural networks[☆,☆☆]

Viola Folli[a], Giorgio Gosti[a,*], Marco Leonetti[a,c], Giancarlo Ruocco[a,b]

[a]*Center for Life Nanoscience,*
Istituto Italiano di Tecnologia,
Viale Regina Elena 291, 00161, Rome, Italy
[b]*Department of Physics,*
Sapienza University of Rome,
Piazzale Aldo Moro 5, 00185, Rome, Italy
[c]*CNR NANOTEC-Institute of Nanotechnology c/o Campus Ecotekne,*
University of Salento, Via Monteroni, 73100 Lecce, Italy

Abstract

We study with numerical simulation the possible limit behaviors of synchronous discrete-time deterministic recurrent neural networks composed of N binary neurons as a function of a network's level of dilution and asymmetry. The network dilution measures the fraction of neuron couples that are connected, and the network asymmetry measures to what extent the underlying connectivity matrix is asymmetric. For each given neural network, we study the dynamical evolution of all the different initial conditions, thus characterizing the full dynamical landscape without imposing any learning rule. Because of the deterministic dynamics, each trajectory converges to an attractor, that can be either a fixed point or a limit cycle. These attractors form the set of all the possible limit behaviors of the neural network. For each network we then determine the

---

[*]Corresponding author

Email addresses: viola.folli@iit.it (Viola Folli), giorgio.gosti@iit.it (Giorgio Gosti), marco.leonetti@roma1.infn.it (Marco Leonetti), Giancarlo.Ruocco@roma1.infn.it (Giancarlo Ruocco)

convergence times, the limit cycles' length, the number of attractors, and the sizes of the attractors' basin. We show that there are two network structures that maximize the number of possible limit behaviors. The first optimal network structure is fully-connected and symmetric. On the contrary, the second optimal network structure is highly sparse and asymmetric. The latter optimal is similar to what observed in different biological neuronal circuits. These observations lead us to hypothesize that independently from any given learning model, an efficient and effective biologic network that stores a number of limit behaviors close to its maximum capacity tends to develop a connectivity structure similar to one of the optimal networks we found.

1. Introduction

Recurrent neural networks are able to store stimuli-response associations, and serve as a model of how live neural networks store and recall behaviors as responses to given stimuli. A discrete-time deterministic recurrent N binary-neuron neural network is completely characterized by its N^2 edges, and its instantaneous state is defined by a neuron activation vector $\boldsymbol{\sigma}$, which is a binary vector of size N. In this paper, we consider a specific kind of recurrent neural network, which is initialized, analogously to a Hopfield network, by assigning to the network's neurons an initial pattern which is the the network stimulus or input. The collection of all possible neuron activation vectors contains 2^N allowed vectors $\boldsymbol{\sigma}$, these vectors can be partitioned in three categories: steady states, limit cycles, and transient states. Steady states are neuron activation states that do not change in time, and limit cycles are sequences of neuron activation vectors that repeat cyclically, with a period that we call cycle length. From now on, we will consider a steady state as a limit cycle of length 1. A network, given any initial activation vector, always evolves to a limit cycle, which for this reason we also refer to as attractor. In other words, a network

associates a limit cycle to any initial neural activation state that is given as an input. For this reason, limit cycles can be considered as behaviors stored as responses to initial stimuli. In the case of length 1 cycles, limit behaviors are a single activation state which in the case of Hopfield networks correspond to the recollection of a memory. In the case of cycles with a length greater than 1, stored limit behaviors are sequences of activation patterns which may correspond to a stored dynamical sequence, such as the performance of a complex motor task, or a dynamic sequence of static memories. In principle, a recurrent neural network stores a certain number of limit behaviors as vectors from a 2^N set in a data structure defined by N^2 parameters. Furthermore, these vectors can be recovered in responses to input stimuli. This clearly has intriguing analogies with content-addressable memory systems capable of indexing large strings of bits (Hopfield, 1987; Carpenter, 1989).

In the past, recurrent neural network, and specifically Hopfield neural networks have been used to model memory storage and recall, though more recently neurobiology models implemented recurrent neural networks to describe brain activity in different cognitive tasks. Mante et al. (2013) use recurrent neural networks to model the integration of context information in the prefrontal cortex in discrimination tasks. Similarly, Carnevale et al. (2015) model with recursive neural networks the premotor cortex modulation of its response criteria in a detection task with temporal uncertainty. Furthermore recurrent neural networks are used to model phoneme acquisition (Kanda et al., 2009), and language acquisition (Heinrich & Wermter, 2018). Neuroscience proposes two fundamental conceptual frameworks that enable recurrent neural networks to store limit behaviors: the connectionist hypotheses and the innate hypotheses. Hebb (1949) proposed the connectionist hypothesis, which assumes that a neural network starts blank and forms new links or adjusts the existing ones each time it stores a new limit behaviors. In this framework limit behaviors are stable equilibria in the neural network dynamics. A criticism of Hebbs' networks is that as new limit behaviors are added the corresponding generated stable states start interfering with the stable states associated with older limit behaviors. This limits

the maximum storage capacity C, which is defined as the maximum number of limit behaviors that can be stored. Notice that this definition is different from the usual definition used in associative memory networks, in which the storage capacity is defined as the number of uniformly distributed random vectors that can be stored in an associative memory (Hassoun, 1993; Hassoun & Watta, 1997). Amit et al. (1985a) shows that a Hebbian network has a storage capacity of $C = pN$ with $p \approx 0.14$. In contrast, innate network models assume that limit behaviors are stored using innate neural assemblies with a given connectivity. Among other innate memory models, Perin et al. (2011) proposes that groups of pyramidal neurons in the rats' neocortex may be innate neuron assemblies that may only partially change their overall connectivity structure. Indeed, Perin et al. (2011) finds that these assemblies have similar connectivity proprieties among different animals, and argues that these assemblies serve as building blocks for the formation of composite complex memories.

Whether we assume a connectionist or an innate network scheme as our working framework, we implicitly assume that a recurrent neural network acts as a content-addressing memory which given an input pattern (stimulus) returns a limit behavior. This limit behavior can be a recovered memory or a more complex neural sequence of neural activations that may be integrated into a second neural network. To understand how well a recurrent neural network acts as a content-addressing memory, the memory storage and retrieval literature uses discrete-time recurrent neural networks with McCulloch-Pitts neurons (McCulloch & Pitts, 1943). Each discrete-time recurrent neural network, which in this literature is sometimes referred to as Hopfield neural network, is characterized by its connectivity matrix $\mathbf{J}$, which schematically represents the set of synapses and electrical junctions connecting couples of neurons. Deterministic discrete-time synchronous recursive neural networks are deterministic discrete dynamical systems. This implies three properties. First, each state in the neural network uniquely transits to another one. Second, the reverse is not true, different states can evolve to the same state. Third, each state belongs to a path that connects it to a stable activity pattern, *i.e.* a limit cycle. Given any

initial neural state, or input, a discrete-time recurrent neural network dynamically falls into an attractor. In this framework, the attractor is the retrieved limit behavior (Hebb, 1949; Amit et al., 1985b; McEliece et al., 1987; Folli et al., 2017; Gutfreund et al., 1988; Bastolla & Parisi, 1998; Sompolinsky et al., 1988; Wainrib & Touboul, 2013). Finally, it is important to consider that a recurrent network associates a limit behavior to each input from the set of all possible N-bit inputs, since the number of limit behaviors C is such that $C << 2^N$, it performs a many-to-few mapping. Recurrent neural network, and in particular the Hopfield model (Hopfield, 1987), show how information can be stored via attractor states. Indeed, there is some experimental support for discrete attractors in the rodents hippocampus cells' activity (Pfeiffer & Foster, 2015), and in monkey cells' activity during tasks (Fuster & Alexander, 1971; Miyashita, 1988).

To understand how well and how many limit behaviors a fully developed neural network can store, we explore how the structure properties of an arbitrary connectivity matrix $\mathbf{J}$ influences the attractor states of the network without imposing an a priori learning rules. Given a connectivity matrix $\mathbf{J}$, to characterize the network structure, we define the network's asymmetry degree ϵ, and dilution degree ρ. The most understood properties on fixed discrete-time recurrent neural networks regard fully-connected Hopfield neural networks. Fully-connected recurrent Hopfield neural networks are networks with dilution degree $\rho = 0$, in which any couple of neurons is connected by two axons one in each direction. In contrast, we define diluted recurrent Hopfield neural networks as networks with $\rho > 0$, in which only a subset of all neurons couples are connected. The existing recurrent Hopfield neural network literature mostly discusses symmetric neural networks in which the weights of the two axons connecting neurons i and j in both directions are the same, and in only few cases researchers investigate asymmetric neural networks $\epsilon > 0$, in which the weights are no longer equal. Furthermore, most of the recurrent Hopfield neural network literature which studies the effect of asymmetry assumes binary neurons with activations state that can take values -1 and $+1$. Under these constraints, it is reported that

5

symmetric fully-connected networks, $\epsilon = 0$, have several attractors, all of which are formed by cycles of length 1 and 2. As the network becomes less symmetric, $\epsilon > 0$, the attractors are composed of longer neural activation patterns. Increasing asymmetry in a fully connected neural network introduces severe drawbacks. Indeed, when the degree of asymmetry is increased above a certain threshold a neural network is subject to a transition from an ordered phase to a "chaotic" regime (Bastolla & Parisi, 1998; Gutfreund et al., 1988). In the chaotic regime, almost identical initial patterns can reach different attractors, and the network is characterized by a high sensitivity to initial conditions. Moreover, this chaotic regime causes exponentially longer recognition time, where the recognition time is the average number of discrete transitions required to reach the corresponding attractor from a generic point in its basin of attraction. Toyoizumi & Huang (2015) analyzes asymetric matrices $\epsilon = 0$ with neuron activation profile $\{-1, 1\}$, and shows that under these conditions as the limit cycle lenght scales exponentialy with N, the number of attractor scales linearly with N. It is important to point out that Bastolla & Parisi (1998), Toyoizumi & Huang (2015), and Gutfreund et al. (1988) discuss synchronous discrete-time recurrent neural networks with single neuron activation profile $\{-1, 1\}$. In this work, we show that these results carry over to neurons with activation profile $\{0, 1\}$. Neurons with activations states $\{0, 1\}$ represent a more accurate model of the single neuron behavior that is observed as either firing or at rest, and how these states determine the excitatory or inhibitory interactions among the neurons in a live neural network. From these evidence, we would argue that symmetric networks, $\epsilon = 0$, are the optimal limiting state for a developing neural network. Nevertheless, most natural neural networks are asymmetric, $\epsilon > 0$ Perin et al. (2011). Therefore, a puzzling contradiction emerges between the observed asymmetry in natural synaptic connections, and the disastrous properties that emerge in fully connected neural network models when the connectivity matrix becomes more asymmetric. Furthermore, in almost all cases live neural networks are not fully connected, $\rho = 0$, but tend to be highly diluted $\rho \sim 0.9$, which implies that not all but just a fraction of neuron couples are connected in the matrix

6

J. For this reason, this paper analyzes not only how the storage properties of neural networks change as we change the asymmetry degree of fully connected connectivity matrices **J**, $\epsilon \in [0, 1]$ and $\rho = 0$. It also studies how the storage properties change as asymmetric connectivity matrices **J** are diluted, $\epsilon = 1$ and $\rho \in [0, 1]$.

Because under certain connectivity conditions we get recurrent neural networks characterized by a minority of attractors with huge attraction basins and a majority of attractors with small attraction basins, almost the entire state space of the neural network is absorbed by few attractors. Consequently, we decided to map the corresponding attractor pattern for each initial network condition. This allows us to explore the entire landscape generated by the complete mapping of all the attractors' basins for different connectivity matrices **J** without losing the attractors with small basins. In addition, we define a way to sample from the space of all connectivity matrices a subset of connectivity matrices **J** with a given asymmetry degree ϵ, and sparsity degree ρ. Thus, we can chart how the attractor landscape properties change sampling connectivity matrices **J** for different values of asymmetry degree ϵ, and sparsity degree ρ. Unfortunately, the computation of the complete transition landscape over all the 2^N initial states is computationally feasible for neural networks up to a certain N. Nevertheless, given these limitations we find the non-trivial result that the symmetric/fully connected region is not the only region with optimal storage capacity, but a second optimal region, the fully-asymmetric/high-dilution region, exists as well. The scaling trends observed in simulations lead us to hypothesize that the results are valid also for values of N larger than the numerical computations we were able to perform. It is surprising to notice that both regions exhibit a similar scaling of the storage capacity even if they have very different connectivity.

Additionally, the values of sparsity and asymmetry, which optimize the number of limit behaviors in discrete-time recurrent neural networks, are found to be remarkably similar to those found in several regions of the mammalian brain that share crucial roles in memory processes. Indeed, the neocortex and the

CA3 region of the hippocampus have been proposed as regions responsible for memory storage (Rolls, 2012), and are clearly diluted (Witter, 2010). The probability of connection between two neocortical pyramidal cells is in the order of 10%, and the probability of connection between two hippocampal CA3 neurons is nearly 4%. While the symmetric/fully optimal connected networks are consistent with the observed live neural networks, the same networks contradict a standard interpretation of Hebbs' Learning, which are noted to tend to the asymmetric/dilute optimal networks. Thus, we are left with the question of why biological networks are found in the fully-asymmetric/high-dilution region. There may be several possible explanations that beg for further investigation. One possibility is that fully connected networks are more costly to develop and maintain in comparison with diluted networks, especially for larger values of N, because for large N there could be important constraints that limit the development of all possible couples of neurons.

The role of dilution in natural neural networks was ignored in past research with the exception of only a couple cases. Theoretical mean field approaches on diluted recurrent neural networks showed weakly correlated firing patterns similar to the patterns observed in the brain cortex (van Vreeswijk & Sompolinsky, 1998; Monteforte & Wolf, 2012). Kim et al. (2017) used simulation to show how, in contrast to fully connected recurrent networks, scale-free networks have an increased number of final behaviors with the side effect of increased errors. Brunel (2016) is an other work that comes to the conclusion that diluted network have optimal storage capacity. This later work investigates the connectivity structure of recurrent neural networks with excitatory synaptic connectivity which are close to their storage limit given a certain degree of retrieval robustness independently from the learning rule. To this aim Brunel (2016) assume that the inhibitory interactions are fully-connected and finds the excitatory matrices that store the greatest number of attractors both analytically with the cavity method and numerically with perceptron learning. Then it investigates the statistical properties of these optimal matrices in large networks. Brunel found that, the optimal excitatory connectivity matrix is diluted, it has several zero-weight

synapses, and that the number of neuron couples with reciprocal connections are greater than in a random network, and that their weight is larger than the average connection weight. Similarly, the approach of this paper is independent of the learning rule, and it searches for the properties of the networks that have optimal storage capacity. Nevertheless, instead of calculating a neural network that can store the maximum number of attractors, it assumes that a network which has reached its storing capacity limit has certain characteristic optimal structures. Thus to find this optimal connectivity structures we can sample sets of connectivity matrices $\mathbf{J}$ with given values of asymmetry ϵ and dilution ρ. Each of these sets will have a characteristic asymmetry degree ϵ and dilution degree ρ and be composed of connectivity matrices $\mathbf{J}$ with certain memory storage properties. From these sets, we can find the values of asymmetry and dilution which characterize the connectivity matrices $\mathbf{J}$ with optimal memory storage properties. Discrete-time recurrent neural networks are minimal models designed to capture the fundamental nature of neural networks, and more realistic models have been proposed (Gerstner, 1998; Maass, 1999; Koch & Segev, 1998; Galves & Löcherbach, 2013). Unfortunately, these models have a necessary additional computational cost which would not allow for such extensive exploration of the attractor landscape associated to connectivity matrices $\mathbf{J}$ at different degrees of dilution and asymmetry.

2. Discrete-Time Recurrent Neural Networks

We consider a network of N binary neurons interacting via a connectivity matrix $\mathbf{J}$, with matrix elements J_{ij} for $i, j = 1, ..., N$. The matrix element J_{ij} represents the strength of the connection between the pre-synaptic neuron j and the post-synaptic neuron i. The state of each neuron is represented by a binary state variable $\sigma_i \in \{0, 1\}$, where $i = 1, \ldots, N$. A neuron σ_i takes values either 0 or 1 if it is respectively at rest (inactive) or firing (active).

2.1. Dynamics

In this section, we introduce a synchronous discrete-time recurrent neural network model with McCulloch-Pitts (McCulloch & Pitts, 1943) neurons. At each time step, all neurons are updated synchronously according to the discrete-time recurrent neural network evolution rule:

$$\sigma_i(t+1) = \theta\Big(\sum_{j=1}^{N} J_{ij}\sigma_j(t) - \eta_i\Big), \tag{1}$$

where $\theta(x)$ is the Heaviside step function ($\theta(x) = 1$ for $x \geq 0$, and $\theta(x) = 0$ otherwise). At the next step $t+1$, the neuron i fires, $\sigma_i(t+1) = 1$, if the summation of its synaptic inputs is above a threshold η_i, otherwise the neuron is inactive, $\sigma_i(t+1) = 0$. In the results discussed in this paper we set $\eta_i = 0$ for all neurons. The vector $\boldsymbol{\sigma}(t) = (\sigma_1(t), \sigma_2(t), \ldots, \sigma_N(t))$ represents the activation profile of all neurons at time t. This activation function emulates the *all-or-none* principle in neuronal activation potentials. The input summation is performed without any scaling on N since the threshold is equal to zero. The scaling factor does not influence the network output that is indeed determined only by the sign of the linear summation. In principle neurons update asynchronously, but Gutfreund et al. (1988), and Nützel (1991) observed that synchronous updating neurons are qualitatively equivalent to asynchronous updating neurons when considering long time scales. Because the objective is to map the full attractor landscape, we have to explore all the possible initial conditions. For this reason, it is fundamental to consider a simplified scheme, and we chose to use a parallel synchronous evolution rule to simplify and speed-up the numerical simulations.

2.2. Content-Addressing Memory Model

A synchronous discrete-time recurrent neural network is a deterministic dynamical system defined on a finite state space. Given any initial neural activation profile $\boldsymbol{\sigma}(0)$ the discrete-time recurrent neural network deterministically evolves in time until it converges to an attractor, which can be composed of a limit cycle composed of a certain number of neural activation states. When

10

a query is submitted to a content-addressing memory we input a search entry and the device returns an address to matching stored data. A discrete-time recurrent neural network works analogously to a content-addressing memory. If the initial neural activation profile $\boldsymbol{\sigma}(0)$ is set equal to an external stimulus, or search entry in the content-addressing memory analogy, then the neural network dynamically converges to an attractor, which represents the retrieved responce. Given this analogy, the limit behavior storage capacity C of a discrete-time recurrent neural network is the number of attractors that are stored in the network.

According to Hebb's rule, memories are added to a Hopfield network by adding to the neural connectivity matrix $\mathbf{J}$ dyadics of the form $\boldsymbol{\sigma}^T\boldsymbol{\sigma}$ (Hebb, 1949). These dyadics generate attractors formed by a length 1 cycle. Thus, in Hebbian learning a memory is a limit behavior composed of a single neural activation profile $\boldsymbol{\sigma}$. Amit et al. (1985a) demonstrated that there is an upper limit to the storage capacity of Hebbian learning networks, and this limit is set to pN with $p \approx 0.14$. This storage capacity upper limit emerges because each time we add a new dyadic term a new attractor is introduced in the Hopfield network dynamics, and at a certain point the new dyadic terms associated with the latest observed attractor interferes with the basin of the old attractors.

In this paper, we use an approach that is independent from the specific learning rule. We assume that, independently from the learning rule, when a discrete-time recurrent neural network stores a number of limit behaviors close to its storing capacity then it approaches characteristic optimal connectivity structures. Thus, instead of packing as many memories as we can in a discrete-time recurrent neural network, and then studying the emergent network structure. We use the total number of attractors to count the number of the network's limit behavior storage capacity. Clearly, some of these attractors may be spurious associations that were not explicitly learned. Consequently, we search for connectivity structures that form the recurrent neural network with the maximum number of attractors. More precisely, we study how many attractors are present in a given arbitrary neural network with a certain connectivity

matrix $\mathbf{J}$ characterized by a specific degree of asymmetry and dilution. Finally, we can study how a recurrent neural network with an optimal connectivity matrix reduces the complexity of the N-dimensional initial problem by clustering the input data in a certain number C of attraction basins.

2.3. Synaptic Matrix

$\mathbf{J}$ is the neural network's connectivity matrix with matrix elements J_{ij}. To analyze the relation between the full attractor landscape and certain global properties of $\mathbf{J}$, we defined a way to generate a random connectivity matrix $\mathbf{J}$ given two fundamental network parameters, respectively the asymmetry coupling degree ϵ, and the sparsity parameter ρ. This section first describes how to generate a random connectivity matrix $\mathbf{J}$ with an arbitrary asymmetry degree ϵ, and fixed sparsity parameter $\rho = 1$, then it describes how to generate a random connectivity matrix $\mathbf{J}$ with arbitrary values of ϵ and ρ.

The elements of a random connectivity matrix J_{ij} with an arbitrary asymmetry degree ϵ and fixed sparsity parameter $\rho = 1$ are generated as the convex sum of the matrix-elements from a symmetric random matrix S_{ij}, and the matrix-elements from a antisymmetric random matrix A_{ij}:

$$J_{ij} = \left(1 - \frac{\epsilon}{2}\right) S_{ij} + \frac{\epsilon}{2} A_{ij}. \tag{2}$$

S_{ij} and A_{ij} are generated with a three-step process. First, the lower diagonal elements of S_{ij} and A_{ij} are randomly drawn from a uniform distribution with greater-than-zero probability in the closed interval $[-1, +1]$. $\mathcal{P}_0(x) = \frac{1}{2}\theta(1-x^2)$ is the distribution from which both the lower diagonal elements of S_{ij} and A_{ij} are drawn, $\mathcal{P}_0(S_{ij})$ and $\mathcal{P}_0(A_{ij})$. Second, the upper diagonal elements are set: $S_{ji}=S_{ij}$ and $A_{ji}=-A_{ij}$. Lastly, the diagonal elements are set to zero: $S_{ii} = 0$ and $A_{ii} = 0$. $J_{ij} = 0$ corresponds to no-connection between i and j, and an J_{ij} element greater or smaller than zero corresponds respectively to an excitatory or an inhibitory connection. For $\epsilon=0$, neurons interact symmetrically with each other; at $\epsilon=1$, J_{ij} is fully-asymmetric. For ϵ ranging from 1 to 2, the strength of antisymmetric couplings increases. In this work, we restrict the analysis for

12

$\epsilon \in [0, 1]$. We set the diagonal elements to zero, $J_{ii}=0$ which implies no autapses (the term autapse indicates a synapse connecting a neuron onto itself).

In order to generate a random connectivity matrix J_{ij} with an arbitrary asymmetry degree ϵ and arbitrary sparsity parameter ρ, we first generate S_{ij} and A_{ij}, and then use Eq. 2 to form J_{ij}. To generate S_{ij} and A_{ij} we draw the elements of the respective lower diagonal elements according to the distribution

$$\mathcal{P}(x) = (1 - \rho)\mathcal{P}_0(x) + \rho\delta(x), \tag{3}$$

where x takes the place of S_{ij} and A_{ij}, and $\delta(x)$ is the Dirac function. $\mathcal{P}(x)$ ensures that the rate of zero-valued elements is determined by the sparsity parameter ρ. Indeed, a random matrix according to this distribution can be generated by drawing S_{ij} and A_{ij} elements from $\mathcal{P}_0(x)$, and then setting each element with probability ρ to zero. In (2), the left term determines the ratio and distribution of non-null elements, and the right term determines the ratio of null elements. Then, the upper diagonal elements are set to $S_{ji}=S_{ij}$ and $A_{ji}=-A_{ij}$, and the diagonal elements are set to zero. Finally, we construct J_{ij} accordingly to (2). This procedure preserves the symmetry and the role of ϵ. Indeed, while $\epsilon = 0$ represents a symmetric matrix with a fraction of zeros on average equal to $\rho + 1/N$, $\epsilon = 1$ indicates a generic, asymmetric, matrix with a number of zeros on average equal to $\rho^2 + 1/N$, which on average is approximately equal to $2\rho - 1 + 1/N$ for ρ close to one. ρ determines how many elements of the matrix are null, and thus the dilution of the neural network connectivity. For $\rho = 0$ we have a fully-connected neural network, in which any two neurons share a synaptic connection in both directions. In the limit for ρ that gets closer to 1, we get a neural network with constantly fewer neural connections, and for $\rho = 1$ we have a network completely lacking any synapses.

2.4. Neural Network Dynamics

Generated a connectivity matrix for a given pair (ϵ, ρ), we evolve all 2^N initial conditions. Being the configuration space finite and the dynamics deterministic, each state $\boldsymbol{\sigma}(t)$ uniquely transits to a state $\boldsymbol{\sigma}(t+1)$. Necessarily, after a transient

13

time, the system relaxes on a limit cycle. Given a certain $\mathbf{J}$, let $\mathcal{G} = (\boldsymbol{\sigma}, T)$ be a directed graph with nodes given by the neurons profiles $\boldsymbol{\sigma}$, and edges T defined as directed couples such that $(\boldsymbol{\sigma}, \boldsymbol{\sigma}') \in T$ if $\boldsymbol{\sigma}$ transits to $\boldsymbol{\sigma}'$. All nodes in $\mathcal{G}$ have one and only one outgoing edge. Let $\mathcal{U}$ be the undirected graph associated to the directed graph $\mathcal{G}$, such that for each $(a, b) \in \mathcal{G}$ there is an undirected couple $\{a, b\} \in \mathcal{U}$. Furthermore, let a weakly connected component of a graph $\mathcal{G}$ be a maximal set of nodes W such that for each couple of nodes $(a, b) \in W$ there is a path that follows the edges in $\mathcal{U}$ and connects a to be b. Since in discrete-time recursive neural networks each initial neuron profile of all the possible 2^N patterns arrives at the corresponding attractor, $\mathcal{G}$ is partitioned in a finite set of C weakly connected components each leading to an attractor (Diestel, 2010). An example of this decomposition is reported in Fig. (1) for a simple N=6 case. This specific network maps 64 possible states into four attractors: two limit cycles with respectively $L = 3, 4$ and two fixed points.

For each weakly connected component k, where $k = 1 \ldots C$, and C is the number of attractors, we measure the following observable variables: (i) the cycle length L_k is the number of states in its attractor, if k is a fixed point $L_k = 1$ or if it is a limit cycles $L_k > 1$; (ii) the basin of attraction size S_k corresponds to the number of states in the k-th weakly connected component; (iii) the average distance D_k between a generic state in the k-th weakly connected component and the corresponding attractor (see table 1).

Table 1: Measured quantities.

Quantity	Description
C	Number of attractors per matrix
L_k	Attractor length
S_k	Basin of attraction size
D_k	Average distance from the attractor

We generate R replicas of the connectivity matrix $\mathbf{J}$ with given ϵ and ρ (up to 100000), and average the values of C, L_k, S_k, and D_k. Then we produce the
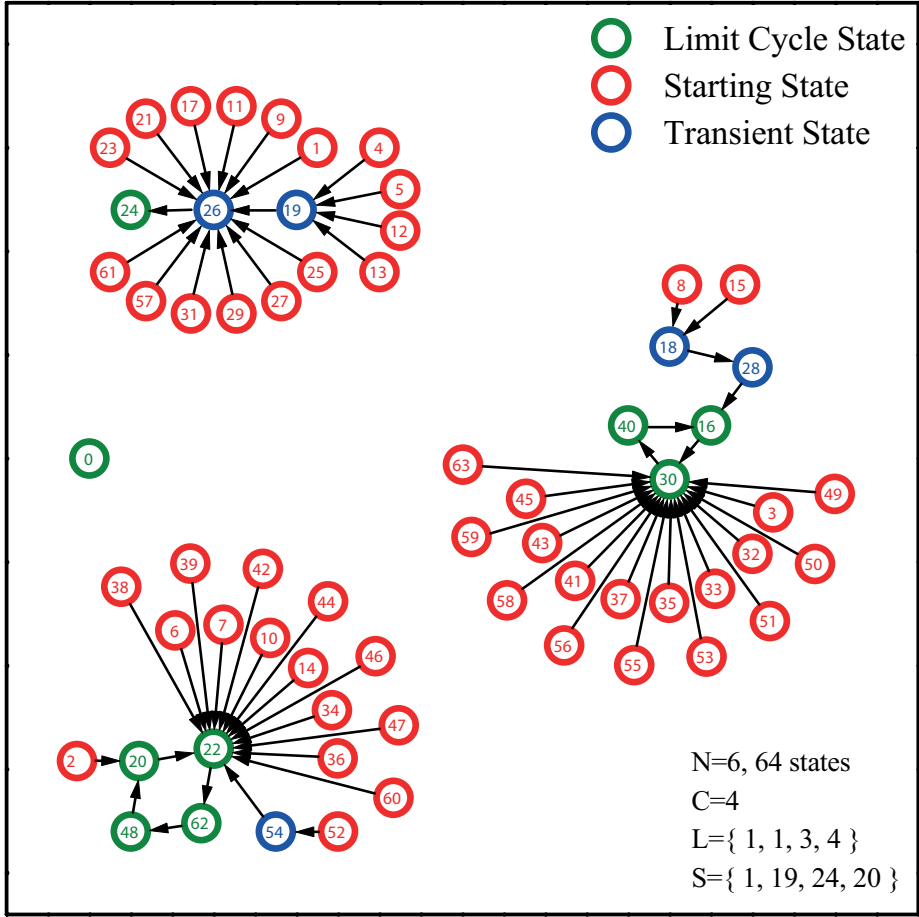
Figure 1: (Color online) Example of weakly connected components of the transition graph $\mathcal{G}$ derived from a given connectivity matrix $\mathbf{J}$. The 2^N numbered circles represents the neural activation profiles $\boldsymbol{\sigma}$. In the present case, N=6, and the connectivity matrix $\mathbf{J}$ is such that ϵ=0 and ρ=0. There are four weakly connected components ($C = 4$), each one containing one attractor, two of them are fixed points, $L_1 = L_2 = 1$, the other are cycles with length L_3 =3 and L_4 =4. The size of their attraction basins are $S_1 = 1$, $S_2 = 19$, $S_3 = 24$, and $S_4 = 20$ respectively. Green circles indicate the points belonging to attractors, while blue and red circles indicate respectively transient and starting points.

histograms $\mathcal{N}(C|\epsilon,\rho)$, $\mathcal{N}(L_k|\epsilon,\rho)$, $\mathcal{N}(S_k|\epsilon,\rho)$, $\mathcal{N}(D_k|\epsilon,\rho)$.

2.5. Large N Limit

All the quantities in table 1 depend on the network size N. Given a network sizes N, we compute the values of these quantities from the complete transition graph $\mathcal{G}$ with all the 2^N neural activation profiles. Thus we measure the scaling of these quantities for different values of N. Because a statistical analysis would be biased by the broad distribution of the basins sizes, we study the complete graph $\mathcal{G}$. Indeed, a few basins are large with size 2^{N-m} where $m \ll N$, and several basins are very small in size. Thus, a statistical analysis would highlight only the trajectories absorbed by the largest basins, given that the probability of selecting the smaller basins is very small. This would result in a under estimation of the number of independent limit cycles. For this reason, it is mandatory to evolve all initial conditions to map the whole landscape of the equilibrium properties of the network. We can complete the analysis only up to a computationally feasible value of N, which turns out to be $N \approx 22$. We have this computational bound because the number of initial conditions scales like 2^N, and the time to evolve all these states and to find the associated attractors scales proportionally to 2^{2N}.

In the numerical results presented in the next section we show that the scaling proprieties of N are mostly preserved across the explored range. Moreover, the functional form and the eventual exponents or multiplicative factors depend on the network parameters (ϵ, ρ). A reasonable question is whether or not the scaling exponents derived from these limited N values can be assumed to be valid in the thermodynamic limit, for large N. To ensure that there are no major changes as N diverges, we have performed a preliminary investigation of the number of cycles of length 1, $\mathcal{N}_1$ for $\rho=0$ and ϵ in the range [0,1]. Tanaka & Edwards (1980) presents a theoretical prediction for this quantity, $\mathcal{N}_1 = e^{\gamma(\epsilon)N}$, with known $\gamma(\epsilon)$ in the infinite size N limit. To test, if the scaling exponent numerically obtained from our simulations with $N < 18$ matches the theoretical infinite size exponent, we compared the estimated $\gamma(\epsilon)$ value, $\hat{\gamma}(\epsilon)$, from our simulations, with the theoretical $\gamma(\epsilon)$ found in Tanaka & Edwards (1980). We found that the two exponents agree within one part per thousand. This result,

though not conclusive, gives us confidence that the finite size estimates of the scaling exponents can be plausible approximations in the large N limit, both in the dense and diluted cases.

Summarizing, this paper focuses on limited size neural networks, this gives us the possibility to exhaustively explore the whole equilibrium landscape and map its changes as symmetry and dilution are varied. A vast amount of literature has been concerned with the analysis of the statistical properties of large neural networks in the thermodynamic limit, using mainly mean-field theories, but little is known about diluted networks. The future objective is to apply the cavity method (Mezard et al., 1987), or the replica method (Gardner, 1988), to analytically determine the number of attractors for diluted connectivity matrices with large N. Thus, we will be able to compare these analytical results with the computational results presented here.

3. Results

In this section, we numerically investigate the attractors' landscape of a discrete-time recurrent neural network for different values of the network size N, the asymmetry degree (ϵ) and the synaptic connectivity dilution (ρ). We report numerical results obtained averaging over $R \sim 10^4$ replica matrices. We start characterizing fully-connected matrices with a specific degree of asymmetry ($\rho = 0$, ϵ). This class of matrices was already investigated analytically, and numerically sampling over the initial conditions, and assuming neuron activation state -1 and 1. Unfortunately, as mentioned earlier sampling on the initial conditions may lead to biased results that miss smaller attractors. Furthermore, we use the more realistic model with neuron activation state 0 and 1. Next, we characterize statistically high-dilution/asymmetric cases, a region that so far has been unexplored.

3.1. Fully Connected Network: from Symmetric to Asymmetric Networks

In figure 2, we report all the quantities listed in table 1 measured for varying ϵ with $\rho = 0$, and the corresponding scaling laws. Here, and in the following,

17

$\langle X \rangle$ indicates an average on X taken over all the attractors, k, and all R replicas of the connectivity matrix $\mathbf{J}$, where X is a quantity from Table 1. As it is shown in (**a**), increasing asymmetry slows down the time required to convergence on the attractor. Thus, as asymmetry increases the stimulus-response time increases. Plot (**b**) shows how $\langle D \rangle$ scales with N and that its trend is well reproduced by a polynomial law. For the mean length of the limit cycles $\langle L \rangle$, we observe two distinct regimes, as clearly presented in panel (**c**) where $\langle L \rangle$ shows a transition around $\epsilon = 0.75$. This transition for discrete-time recurrent neural networks with neuron activation states $\sigma_i \in \{0, +1\}$ is analogous to the transition observed in recurrent neural networks with $\sigma_i \in \{-1, +1\}$ (Gutfreund et al., 1988). Correspondingly, the scaling law (**d**) displays a rather sharp transition from an ordered phase where

$$\langle L \rangle \sim N^{\gamma_p} \tag{4}$$

to a chaotic regime, in which the mean length of limit cycles increases exponentially with the system size N:

$$\langle L \rangle \sim 2^{\gamma_e N}. \tag{5}$$

An exponentially long limit cycle length means that for large N, the network displays longer attractors with seemingly aperiodic behavior (the network dynamics appears to be chaotic).

In panels e and g, we report the mean values of the number of attractors per matrix, $\langle C \rangle$, and of the basins of attraction size $\langle S \rangle$ for fully-connected matrices, $\rho = 0$. It is clearly evident how the network loses the capacity to cluster the input data in sub-domains as ϵ is increased: the number of attractors $\langle C \rangle$ is drastically reduced and correspondingly the dimension of the basins increases. The state space tends to be subdivided into a small number of large regions, each with its attractor, and the network is no longer able to distinguish different inputs. The average number of attractors scales exponentially for $\epsilon = 0$ (panel f). For fully-connected matrices, $\rho = 0$, and $\epsilon = 0$, $\langle C \rangle \sim 2^{\gamma_e N}$ with $\gamma_e = 0.28$. For $\rho = 0$, and $\epsilon = 1$, the number of attractors scales polynomially, as expected
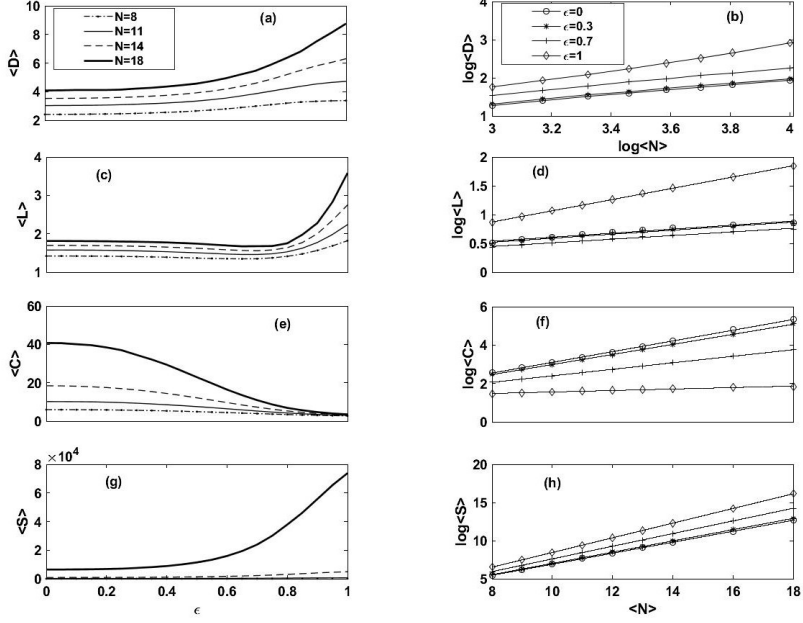
Figure 2: The panels on the left column report the averaged quantities in Table 1 as a function of the asymmetry degree ϵ for $N = 8, 11, 14, 18$. The panels on the right column display the corresponding scaling laws with the system size N for $\epsilon = 0, 0.3, 0.7, 1$. (**a**) Increasing the asymmetry slows down the convergence time $\langle D \rangle$ to the attractor, the corresponding scaling law (**b**) is polynomial with N. (**c**) The asymmetry produces the emergence of limit cycles with length $L > 2$, at $\epsilon \sim 0.75$ the averaged $\langle L \rangle$ increases exponentially $\sim 2^{\gamma N}$ with exponent $\gamma = 0.1$ (**d**), which indicates exponentially long limit cycles. (**e-f**) Increasing asymmetry in fully connected neural networks leads to a drastic reduction of the number of attractors which develop larger basins (**g-h**). This implies a loss of computational ability, because for larger ϵ the network becomes unable to cluster the input data in sub-domains.

from Toyoizumi & Huang (2015) analysis. In $\langle C \rangle$, there is probably a transition as for the attractor length $\langle L \rangle$. Panel (h) shows the scaling of $\langle S \rangle$. For fully-connected matrices, $\rho = 0$, $\langle S \rangle$ has an inverse behavior compared to $\langle C \rangle$, $\langle S \rangle$ scales exponentially for $\epsilon = 1$, and it scales polynomially for $\epsilon = 0$. Increasing asymmetry causes the network to develop a glassy behavior, the network is greatly slowed down and unable to quickly recognize the attractor of a given input. The higher the asymmetry degree, the higher the probability that the

system admits only one attractor with a basin 2^N states large, the network loses its capacity to deal with "complexity". In conclusion, although asymmetry in synaptic connection is a property of biological networks, asymmetry in dense networks is not sufficient to realize a network capable of storing and retrieving stimulus response associations. We now investigate the interplay between asymmetry and sparsity and how the dilution helps asymmetric networks to store more memories.

3.2. From Fully-Connected to Diluted Asymmetric Networks

A diluted and asymmetric discrete-time recurrent neural network recovers an optimal storage capacity and stimulus-response association time compared to a dense asymmetric recurrent neural network. Greater dilution increases the number attractors and accelerates the retrieval process. Here, we analyze the same quantities measured in the previous section, but we consider different dilution values $\rho \in (0,1)$, and keep constant the asymmetry coefficient ϵ=1. Thus, we consider asymmetric networks at different dilution levels. In figure 3, we report how the convergence time D changes with the dilution ρ (**a**) and how it scales with N (**b**). Increasing dilution ρ drastically decreases the average stimulus-response association $\langle D \rangle$ for pattern retrieval. In other words, the dilution improves the ability of the network to converge to an attractor. Figure 3 (**c**) shows how as dilution increases the length of limit cycles is reduced. In highly diluted systems (ρ above 0.7), a polynomial fit better predicts the observed data compared to an exponential fit (**d**). The scaling coefficient is γ_p=0.66±0.07 for ρ=0.95. In other words, for diluted networks the limit cycles length does not scale exponentially with N anymore, and the "chaotic" regime ceases.

Figure 4 reports the main result of the present work. It provides direct evidence of the nontrivial effect of dilution: increasing dilution in an asymmetric network causes the appearance of an unexpected maximum for the storage capacity $\langle C \rangle$ at ρ=0.95 (**a**). This value approximately corresponds to 90% of zeros in the synaptic matrix, meaning only 10% of the neuron pairs are connected. The height of the peak exponentially scales with the network size N (**b**)
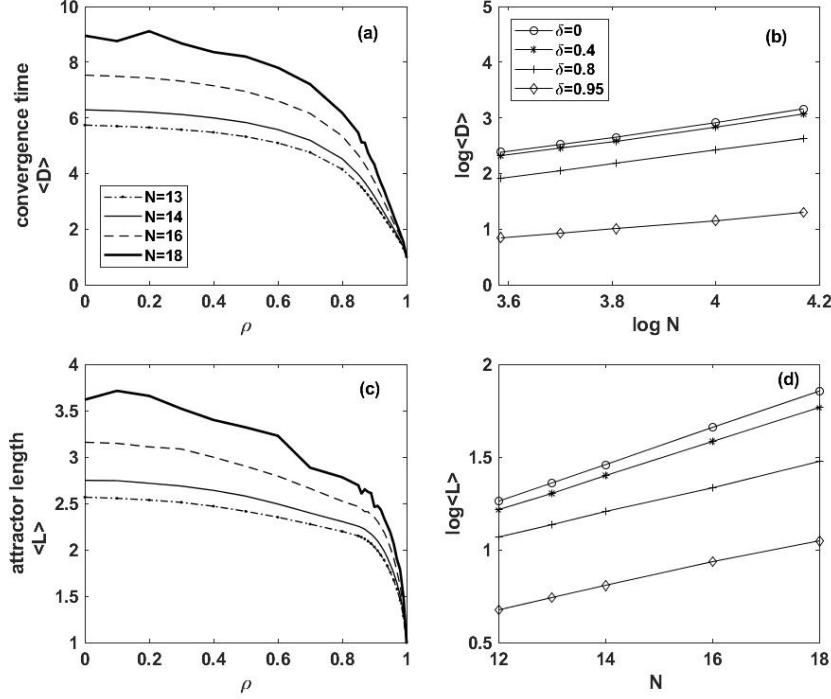
Figure 3: The panels on the left, (**a**) and (**c**), show respectively how the average convergence time $\langle D \rangle$ and the average limit cycle length $\langle L \rangle$ change over different ρ values given $N = 13, 14, 16, 18$. The panels on the right, (**b**) and (**d**), show how $\langle D \rangle$ and $\langle L \rangle$ scale over different N values given $\rho = 0, 0.4, 0.8, 0.95$. **Increasing sparsity in asymmetric matrices reduces the convergence time and the attractor lengths. Thus, sparse matrices recover computation ability and lose exponentially long limit cycles characteristic of the chaotic regime.**

with γ_e=0.28±0.02 for ρ=0.95, which is approximately the same scaling value estimated for $\langle C \rangle$ in fully-connected symmetric networks with ϵ=0, ρ=0.

A caveat is due because finite size effects may determine the emergence of the peak. Indeed, it is unclear, given the current observations, if, for large N, the peak position around ρ=0.95 is stable or if it drifts towards ρ=1 (finite size effect). For this purpose, possible future investigation could be the analytical estimation of the peak position given the thermodynamic limit, which may
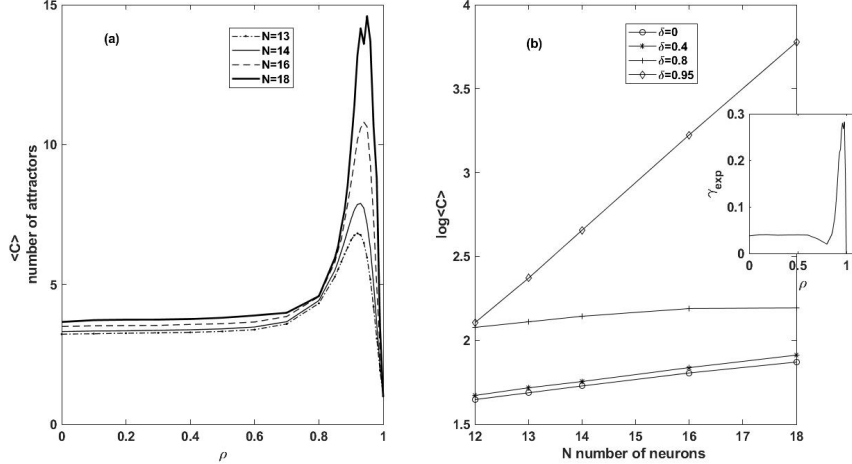
Figure 4: (**a**) The plot shows how $\langle C \rangle$ changes with the dilution coefficient ρ for different values of N, $N = 13, 14, 16, 18$. (**b**) The plot shows how $\langle C \rangle$ scales with N for $\rho = 0, 0.4, 0.8, 0.95$. The inset shows the exponential coefficients for different values of ρ. **The figure reports the main result of the present work. As sparsity in fully asymmetric matrix is increased, an optimal region appears: the non-monotonic peak in which the network architecture admits an exponentially large number of attractors. Furthermore, as shown in Fig. 3, in the same regime, the network is able to quickly recall memories converging to the corresponding attractor, and the attractor is generally a limit cycle with small L. All these features show an optimal asymmetric/diluted network regime that maximizes the storage capacity and the recovery efficiency.**

be obtained with the replica method or the more appropriate cavity method Mezard et al. (1987). It is important to point out that if it is actually true that the peak drifts and disappears in the thermodynamic limit, this implies that its maximum position gets closer and closer to the "empty" matrix value ρ=1. Given that the peak height will most likely increase exponentially with N, we would find that an exponential number of stimulus-response associations could be stored in almost-connection-free large networks.

To qualitatively validate the persistence of the peak for large networks, we implemented a Monte Carlo experiment that estimates the average number of

attractors $\langle C \rangle$ for networks with $N = 45$, $\epsilon = 1$ and for $0 \leq \rho \leq 1$. For each network, we sampled 2^8 initial conditions out of 2^{45}, thus we explore a fraction equal to 10^{-11} of the entire initial condition space. This estimate is biased differently depending on the network's specific values of symmetry ϵ and dilution ρ, because for certain values of symmetry ϵ and dilution ρ we have a different distribution of the size of the attraction basins, which produces a disproportion in the sampling probability of attractors with small attraction basins. For $N = 45$, we find that the peak at $\rho = 0.95$ is preserved, but that the value of $\langle C \rangle$ relatively raises for $\rho \ll 0.8$ compared to $\rho \gg 0.8$, because for $\rho \ll 0.8$, $\langle C \rangle$ is overestimated with regards to the estimate at $\rho \gg 0.8$. This indicates the random sampling inapplicability and the need for an exhaustive scan of the initial condition. Furthermore, this observation reinforces the hypothesis that for large N the peak persists around $\rho = 0.95$.
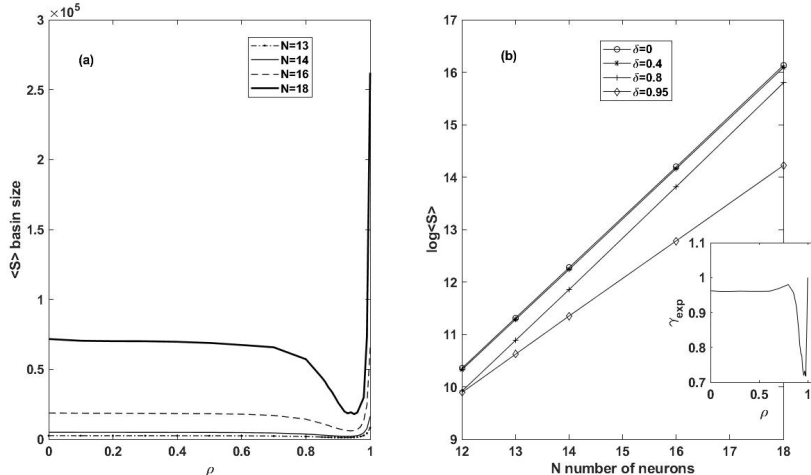

Figure 5: (a) The plot shows how the average basin size $\langle S \rangle$ changes as a function of the dilution parameter ρ for different values of N, $N = 13, 14, 16, 18$. (b) Shows how $\langle S \rangle$ scales with N for $\rho = 0, 0.4, 0.7, 0.95$. The insert shows the exponential scaling coefficients for different ρ values. **This figure shows that the region with the maximum storage capacity is characterized by many small attraction basins.**

Figure 5 shows how the average basin size $\langle S \rangle$ changes as a function of the

dilution and of the network size N. In correspondence of the peak in $\langle C \rangle$, the dimension of the attraction basins decreases (see figure 5 (**a**)). The state space tends to be subdivided in a large number of small regions, each with its attractor. This and the fast stimulus-response association tells us that the network is able to quickly subdivide the inputs in clusters: in fact, at ρ=0.95, the average convergence time is strongly reduced with respect to the chaotic regime and its scaling turns from exponential to polynomial (see figure 3, (**a**)-(**b**)). All these observations allow us to conclude that asymmetric-diluted recurrent neural networks exhibit optimal information processing and memory storage for ρ=0.95 and ϵ=1.

4. Discussion

This paper discusses how the dilution and asymmetry of a discrete-time recurrent neural network connectivity matrix **J** influences the network's limit behavior storage capacity and its response time. More precisely, it explores the effect of dilution in a discrete-time recurrent neural network of binary neurons with an asymmetric excitatory/inhibitory connectivity matrix. Given an arbitrary learning rule, and an incremental sequence of memories, a recurrent neural network, reaches a limit behavior storage limit. We suppose that this limit is in general characteristic of the particular learning rule. To go beyond the limitation of having to assume a particular learning rule, we consider the recurrent neural network limit behavior storage capacity as the upper bound of the limit behavior storage capacity of any arbitrary learning rule. Furthermore, we assume that the connectivity matrix of a recurrent neural network which has stored a number of limit behaviors close to the storage limit must have a connectivity matrix characterized by a specific structure with certain values of asymmetry and dilution. Clearly, this characteristic connectivity structure must approach the structure of a recurrent neural network with the largest number of attractors obtained from a pool of all possible networks, because this should be equivalent to the network that has potentially stored the largest number of

memory vectors. To find this characteristic storing structure, we sample random connectivity matrices $\mathbf{J}$ of arbitrary asymmetry ϵ and dilution ρ, and for each matrix we map the full attractor basin for all 2^N initial conditions. This allows us to examine the neural network's storage capacity, and measure how quickly it clusters 2^N initial conditions into the corresponding attractors. We considered the scenario in which the network is potentially able to store memories both as fixed point attractors and limit cycles attractors, without imposing any a priori learning role.

We found two regions in the asymmetric/diluted space (ϵ, ρ) of all possible sampled networks in which neural networks exhibit optimal storage capacity. The first optimal storage capacity region contains asymmetric $\epsilon = 1$ and diluted $\rho \sim 0.95$ connectivity matrices. This means that a large fraction ($\sim 90\%$) of elements in the connectivity matrix are zero. The second optimal region incorporates fully-symmetric $\epsilon = 0$, and fully connected matrices $\rho = 0$, in this region almost all connectivity matrix elements are non-null. Similar connectivity as in the first region is observed in the neocortex and in the CA3 region of the hippocampus (Witter, 2010; Perin et al., 2011). These natural neural networks are implicated in memory storage and retrial. These observations are coherent with previous analytical and computational observations (Kim et al., 2017; van Vreeswijk & Sompolinsky, 1998; Monteforte & Wolf, 2012), but it was unknown how this optimal connectivity changes in the surrounding of the optimal value of ρ and was considered as substantial evidence against Hebbian learning. For this reason Hebbian learning is considered as a poor model of learning in animal neural networks. Contrarily, the second region is only predicted by Hebbian learning but is not observed in natural neural networks. Furthermore, we found that in the fully-connected $\rho = 0$ and fully-asymmetric region $\epsilon = 1$, the recurrent neural networks exhibit a very low storage capacity, and large basins of attraction, which implies that the network is no longer able to distinguish and separate different external stimuli. In addition, fully-connected and asymmetric regions have very long (glassy) recognition times, which compromise the ability of the recurrent neural network to respond to external stimuli. From a neurobi-

ological prospective, this means that when a recurrent neural network drifts out of its optimal state for some external cause such as a disease, then the network becomes less effective in separating different stimuli, and discriminating errors from signals. In addition, its response times become longer. In line with these observations, Tang et al. (2014) report that the brain of patients affected by autism spectrum disorders (ASDs) presents an altered connectivity, or dilution, compared to healthy individuals, and specifically reports an alteration in the neocortex connectivity. Suppose that the brain regions involved in ASDs are displaced from their optimal asymmetric/diluted region, we could argue, given our observations, that this displacement may cause a disruption of the ability to separate different stimuli in distinct responses, and produce longer response times.

5. Conclusion

From our exploration of the role of connectivity and symmetry in recursive neural networks, we find two regions that optimize limit behavior storage and signal-response association. The first region is composed of asymmetric/diluted networks, and the second region is formed of symmetric/fully-connected networks. Furthermore, we found a third region made of asymmetric/fully-connected networks characterized by chaotic and glassy limit behaviors. From these results we are left with the question of why adaptation and evolution selected the first region. Is this because more non-zero elements in the connectivity matrix corresponds to more costly connections? Is it because fully-connected networks imply the existence of two axons between any two neurons and this would be spatially impossible if not technically implausible for large network sizes N? Is it because the natural learning rules that guide neural networks development force them to dynamically evolve in the second region?

Lastly, to partly overcome the smallness of N, we have also analyzed the scaling properties of the main measured quantities. We have found that the scaling behavior for the averaged number of length 1 cycles in fully-connected

symmetric networks are perfectly in agreement with theoretical values found by Tanaka & Edwards (1980). Thus the averaged number of length 1 cycles is not biased by the finite size effects. In addition, in the analyzed range for small N, all the scaling laws appear highly robust. These observations do not guarantee that the same occurs for the scaling laws of other observable quantities in diluted networks. Nevertheless, it gives us confidence in the extrapolation of the scaling laws observed in this paper.

Conflict of Interest Statement

The authors declare that the research was conducted in the absence of any commercial or financial relationships that could be construed as a potential conflict of interest.

References

References

Amit, D. J., Gutfreund, H., & Sompolinsky, H. (1985a). Spin-glass models of neural networks. *Physical Review A*, *32*, 1007–1018.

Amit, D. J., Gutfreund, H., & Sompolinsky, H. (1985b). Storing infinite numbers of patterns in a spin-glass model of neural networks. In *Spin Glass Theory and Beyond: An Introduction to the Replica Method and Its Applications.* (pp. 428–431).

Bastolla, U., & Parisi, G. (1998). Relaxation, closing probabilities and transition from oscillatory to chaotic attractors in asymmetric neural networks. *Journal of Physics A: Mathematical and General*, *31*, 4583–4602.

Brunel, N. (2016). Is cortical connectivity optimized for storing information? *Nature Neuroscience*, *19*, 749–755.

Carnevale, F., deLafuente, V., Romo, R., Barak, O., & Parga, N. (2015). Dynamic Control of Response Criterion in Premotor Cortex during Perceptual Detection under Temporal Uncertainty. *Neuron*, *86*, 1067–1077.

Carpenter, G. A. (1989). Neural network models for pattern recognition and associative memory. *Neural Networks*, *2*, 243–257.

Diestel, R. (2010). *Graph Theory*. Springer-Verlag Berlin Heidelberg.

Folli, V., Leonetti, M., & Ruocco, G. (2017). On the Maximum Storage Capacity of the Hopfield Model. *Front. Comput. Neurosci*, *10*, 144.

Fuster, J. M., & Alexander, G. E. (1971). Neuron Activity Related to Short-Term Memory. *Science*, *173*, 652–654.

Galves, A., & Löcherbach, E. (2013). Infinite Systems of Interacting Chains with Memory of Variable Length-A Stochastic Model for Biological Neural Nets. *Journal of Statistical Physics*, *151*, 896–921.

Gardner, E. (1988). The space of interactions in neural network models. *Journal of Physics A: General Physics*, *21*, 257–270.

Gerstner, W. (1998). Populations of spiking neurons. *Pulsed Neural Networks*, *1*, 261–295.

Gutfreund, H., Reger, J. D., & Young, A. P. (1988). The nature of attractors in an asymmetric spin glass with deterministic dynamics. *Journal of Physics A: Mathematical and General*, *21*, 2775.

Hassoun, M. H. (1993). *Associative neural memories : theory and implementation*. Oxford University Press.

Hassoun, M. H., & Watta, P. B. (1997). Associative memory networks. In E. Fiesler, & R. Beale (Eds.), *Handbook of Neural Computation*, chapter 14. Taylor & Francis Group.

Hebb, D. (1949). *The Organization of Behavior*. New York: Wiley.

28

Heinrich, S., & Wermter, S. (2018). Interactive natural language acquisition in a multi-modal recurrent neural architecture. *Connection Science*, *30*, 99–133.

Hopfield, J. J. (1987). Neural networks and physical systems with emergent collective computational abilities. In *Spin Glass Theory and Beyond: An Introduction to the Replica Method and Its Applications* (pp. 411–415).

Kanda, H., Ogata, T., Takahashi, T., Komatani, K., & Okuno, H. G. (2009). Phoneme acquisition model based on vowel imitation using Recurrent Neural Network. In *2009 IEEE/RSJ International Conference on Intelligent Robots and Systems* (pp. 5388–5393). IEEE.

Kim, D.-H., Park, J., & Kahng, B. (2017). Enhanced storage capacity with errors in scale-free Hopfield neural networks: An analytical study. *PLOS ONE*, *12*, e0184683.

Koch, C., & Segev, I. (1998). Methods in Neuronal Modeling: From Ions to Networks. *Computational neuroscience*, *2*, 1–26.

Maass, W. (1999). Computing with Spiking Neurons. *Pulsed Neural Networks*, (pp. 55–85).

Mante, V., Sussillo, D., Shenoy, K. V., & Newsome, W. T. (2013). Context-dependent computation by recurrent dynamics in prefrontal cortex. *Nature*, *503*, 78–84.

McCulloch, W. S., & Pitts, W. (1943). A logical calculus of the ideas immanent in nervous activity. *The Bulletin of Mathematical Biophysics*, *5*, 115–133.

McEliece, R. J., Posner, E. C., Rodemich, E. R., & Venkatesh, S. S. (1987). The Capacity of the Hopfield Associative Memory. *IEEE Transactions on Information Theory*, *33*, 461–482.

Mezard, M., Parisi, G., & Virasoro, M. A. (1987). *Spin glass theory and beyond*. World Scientific.

Miyashita, Y. (1988). Neuronal correlate of visual associative long-term memory in the primate temporal cortex. *Nature*, *335*, 817–820.

Monteforte, M., & Wolf, F. (2012). Dynamic flux tubes form reservoirs of stability in neuronal circuits. *Physical Review X*, *2*, 041007.

Nützel, K. (1991). The length of attractors in asymmetric random neural networks with deterministic dynamics. *Journal of Physics A: Mathematical and General*, *24*, L151.

Perin, R., Berger, T. K., & Markram, H. (2011). A synaptic organizing principle for cortical neuronal groups. *Proceedings of the National Academy of Sciences*, *108*, 5419–5424.

Pfeiffer, B. E., & Foster, D. J. (2015). Autoassociative dynamics in the generation of sequences of hippocampal place cells. *Science*, *249*, 180–183.

Rolls, E. T. (2012). Advantages of dilution in the connectivity of attractor networks in the brain. *Biologically Inspired Cognitive Architectures*, *1*, 44–45.

Sompolinsky, H., Crisanti, A., & Sommers, H. J. (1988). Chaos in random neural networks. *Physical Review Letters*, *61*, 259.

Tanaka, F., & Edwards, S. F. (1980). Analytic theory of the ground state properties of a spin glass. I. Ising spin glass. *Journal of Physics F: Metal Physics*, *10*, 2769–2778.

Tang, G., Gudsnuk, K., Kuo, S.-H., Cotrina, M., Rosoklija, G., Sosunov, A., Sonders, M., Kanter, E., Castagna, C., Yamamoto, A., Yue, Z., Arancio, O., Peterson, B., Champagne, F., Dwork, A., Goldman, J., & Sulzer, D. (2014). Loss of mTOR-Dependent Macroautophagy Causes Autistic-like Synaptic Pruning Deficits. *Neuron*, *83*, 1131–1143.

Toyoizumi, T., & Huang, H. (2015). Structure of attractors in randomly connected networks. *Physical Review E*, *91*, 032802.

van Vreeswijk, C., & Sompolinsky, H. (1998). Chaotic Balanced State in a Model of Cortical Circuits. *Neural Computation*, *10*, 1321–1371.

Wainrib, G., & Touboul, J. (2013). Topological and dynamical complexity of random neural networks. *Physical Review Letters*, *110*, 118101.

Witter, M. P. (2010). Connectivity of the Hippocampus. In *Hippocampal Microcircuits* (pp. 5–26).